Supporting Information

Overcoming the challenges associated with InN/InGaN heterostructure via nanostructuring approach for broad band photodetection

Arun Malla Chowdhury, [*,1,2] *Deependra Kumar Singh,*[1] *Basanta Roul,*[1, 3] *K K Nanda*[*,1] *and S B Krupanidhi*[*,1]

1. Materials Research Centre, Indian Institute of Science, Bangalore-560012, India.
2. Department of Physics, Syamsundar College, University of Burdwan, East Bardhaman, West Bengal 713424, India.
3. Central Research Laboratory, Bharat Electronics, Bangalore 560013, India.

Corresponding Authors

*E-mail: nanda@iisc.ac.in

*E-mail: sbk@iisc.ac.in

*Email: amchowdhury@iisc.ac.in

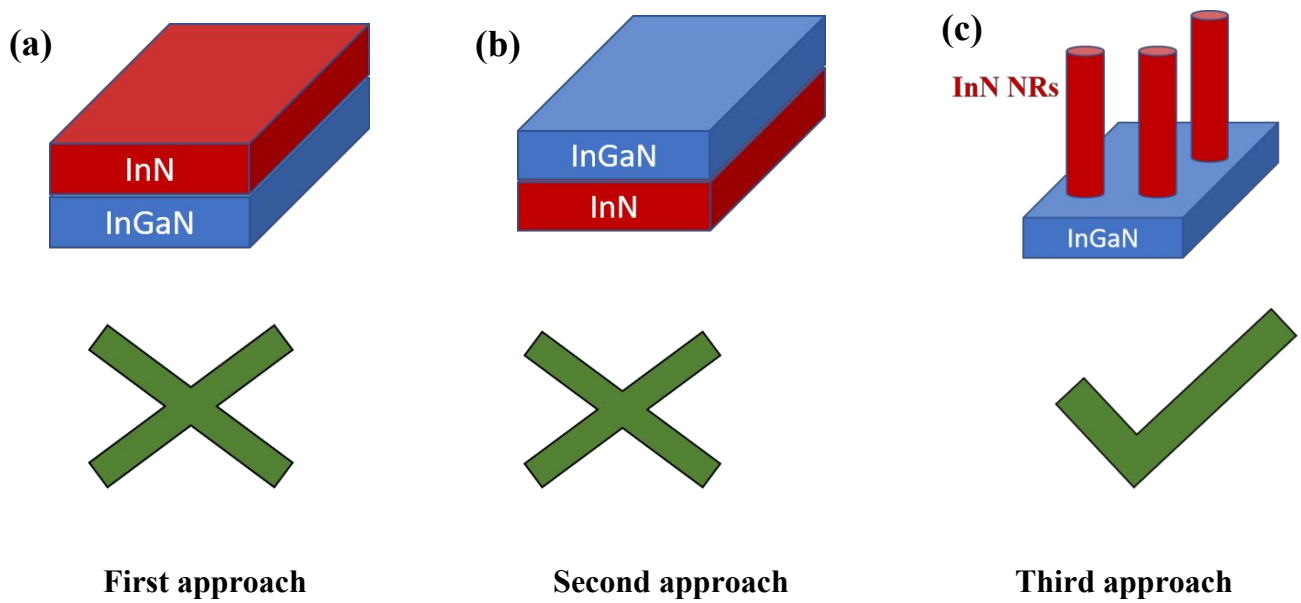

Figure S1. Structure development for UV, visible and infrared light detection with InN and InGaN (a, b) first and second approaches (not acceptable). (c) third approach (accepted).

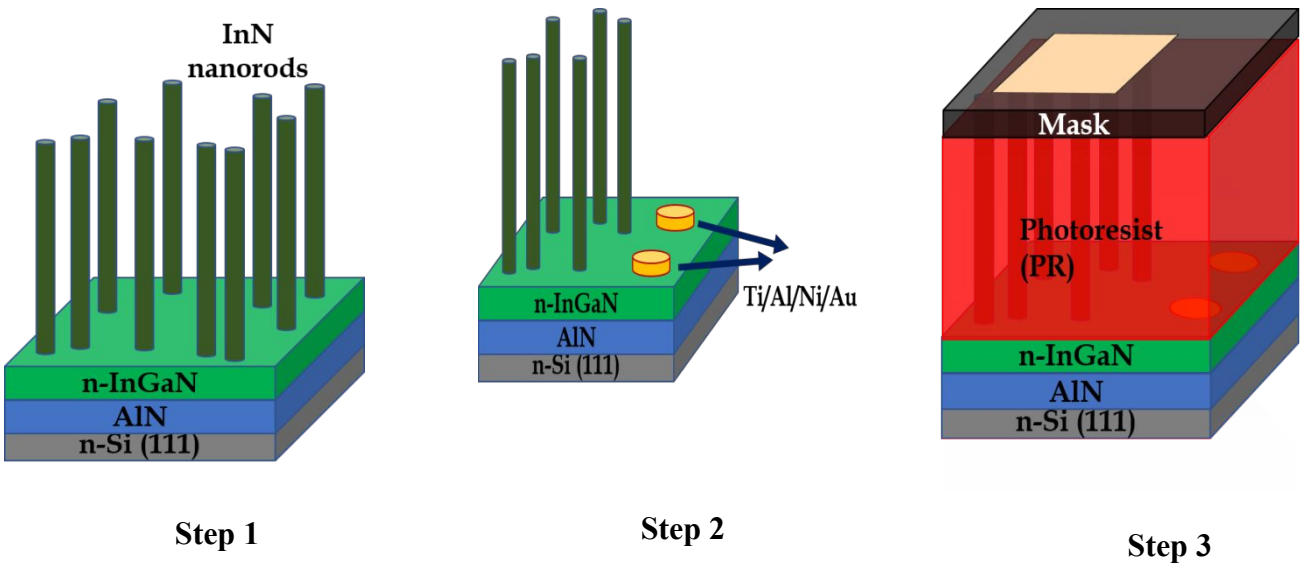

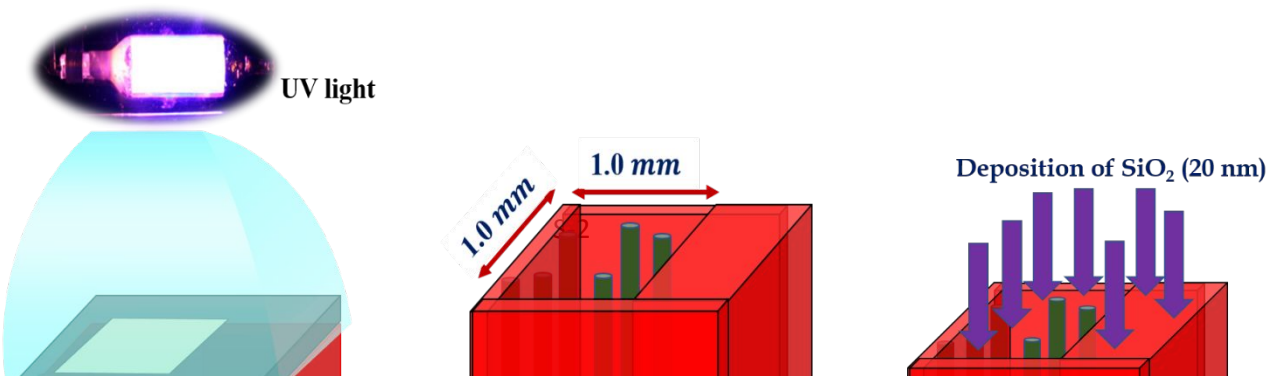

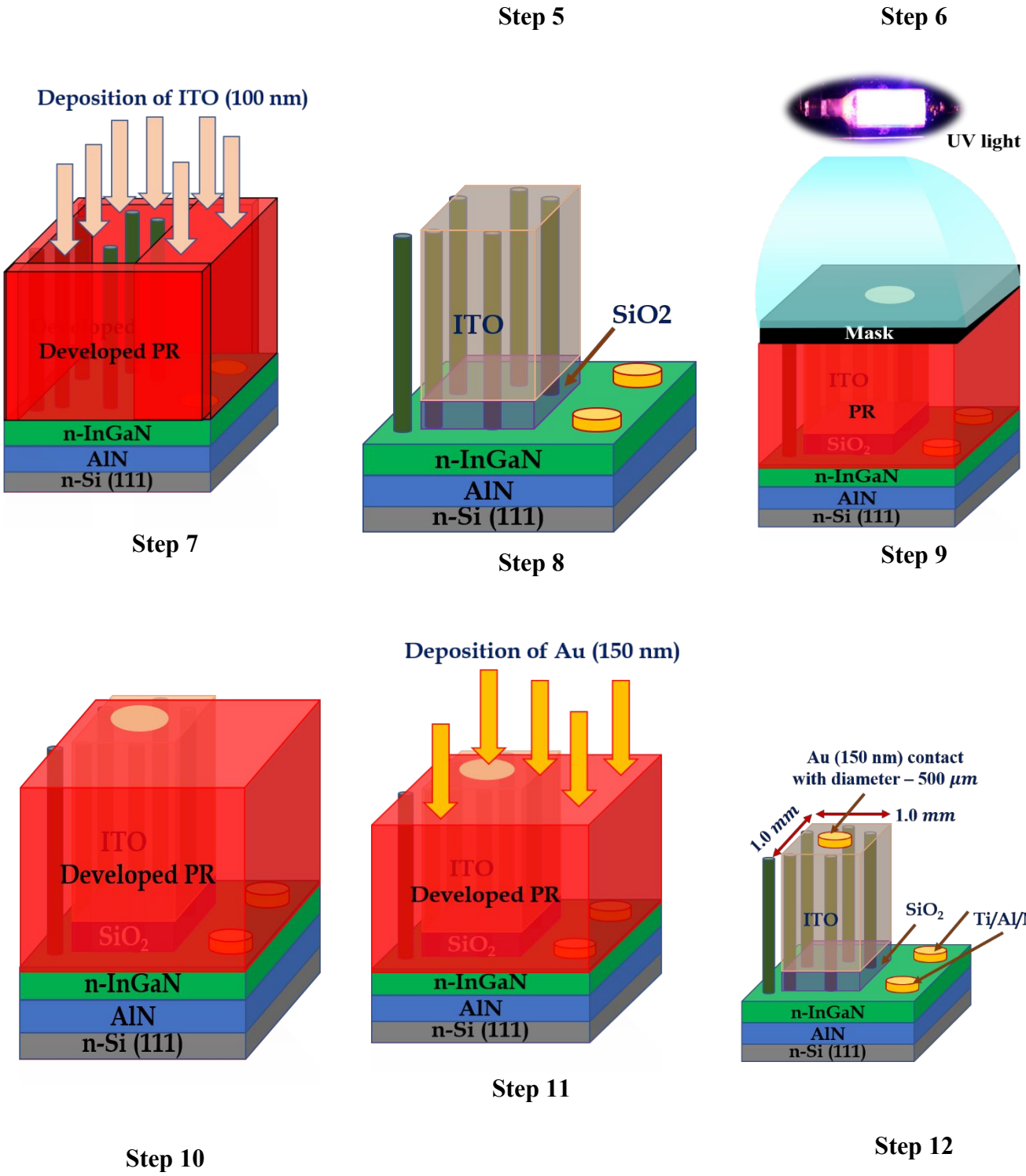

Figure S2. Schematic diagram of device processing.

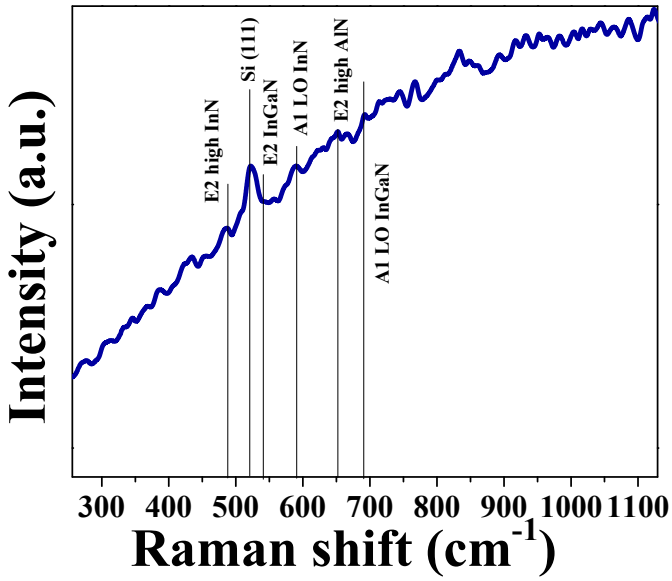

Figure S3: Room temperature Raman spectrum of the heterostructure with 532 nm.

The peaks obtained from Raman spectra are E2 high InN (489 cm^{-1}), Si (111) (520.5 cm^{-1}), E2 InGaN (538 cm^{-1}), A1 LO InN (591 cm^{-1}), E2 high AlN (653 cm^{-1}) and A1 LO InGaN (691 cm^{-1})[1–3]. The overall increase in the Raman peak indicates the background noise and it has been reported in various literature[4,5].

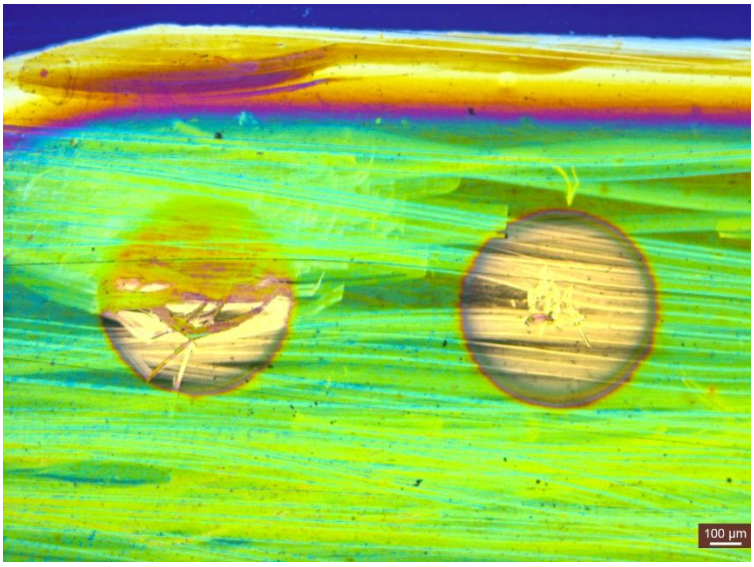

Figure S4: Asymmetry contact area image on the top of InGaN epilayer by optical microscope.

It is clearly seen from Figure S4 that the contacts on InGaN layer is uneven. One contact is almost circular and another one is half circular. Hence, this asymmetry in contact area leads the photocurrent even at zero bias. When the photogenerated carriers are generated between the two electrodes, the carriers are equally likely to be collected by both the electrodes. But the contact, which is having larger area, collects more photogenerated carriers than the other one. Therefore, photocurrent can be observed at zero bias from InGaN epilayer only due to the uneven collection of photogenerated carriers by both the electrodes.

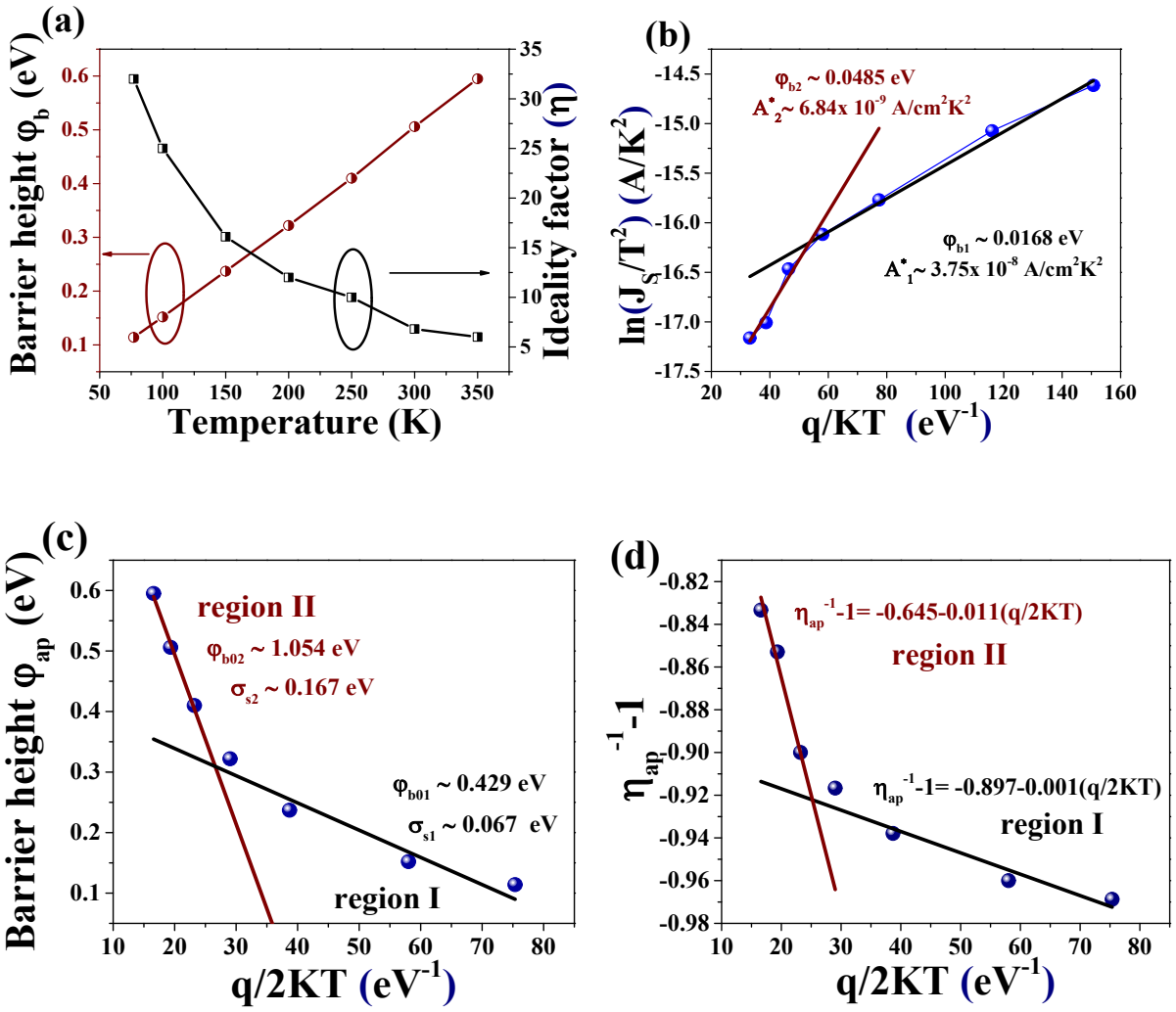

Figure S5. (a) The derived values of barrier height and ideality factor from temperature dependent *J-V* characteristics. (b) The conventional Richardson's plot. (c) φ_{ap} vs $\frac{q}{2KT}$. (d) $\left(\eta_{ap}^{-1}-1\right)$ vs $\frac{q}{2KT}$.

Table S1: Parameters obtained according to TE model from temperature dependent

J-V characteristics.		
Temperature (K)	φ_b**(eV)**	η
77	0.114	32
100	0.152	25
150	0.237	16.1
200	0.322	12
250	0.410	10
300	0.506	6.8
350	0.595	6

Table S2: Parameters obtained from equation 7 and 8.				
	region I (77 – 200 K)		**region II (250 – 350 K)**	
equation 7	$\overline{\varphi}_{b01}$ **(eV)**	σ_{s1} **(eV)**	$\overline{\varphi}_{b02}$ **(eV)**	σ_{s2} **(eV)**
	0.429	0.067	1.054	0.167
equation 8	ρ_2 **(V)**	ρ_3 **(V)**	ρ_2 **(V)**	ρ_3 **(V)**
	-0.897	0.001	-0.645	0.011

Table S3: Parameters obtained from modified Richardson's plot.			
region I (77 – 200 K)		**region II (250 – 350 K)**	
$\overline{\varphi}_{b0}$	A^*	$\overline{\varphi}_{b0}$	A^*
0.43 eV	18.17 A/cm^2K^2	1.05 eV	11.59 A/cm^2K^2

Bibliograohy:

(1) Hsu, L.; Lin, C.; Hwang, Y.; Su, C.; Lin, S. Optical Properties of InN-Based Photo Detection Devices. **2015**, 15–18.

(2) Liu, L.; Liu, B.; Edgar, J. H.; Rajasingam, S.; Kuball, M. Raman Characterization and Stress Analysis of AlN Grown on SiC by Sublimation. *J. Appl. Phys.* **2002**, *92* (9), 5183–5188.

(3) Alexson, D.; Bergman, L.; Nemanich, R. J.; Dutta, M.; Stroscio, M. A.; Parker, C. A.; Bedair, S. M.; El-Masry, N. A.; Adar, F. Ultraviolet Raman Study of A1(LO) and E2 Phonons in InxGa1-XN Alloys. *J. Appl. Phys.* **2001**, *89* (1), 798–800.

(4) Finnie, P.; Ouyang, J.; Lefebvre, J. Full Spectrum Raman Excitation Mapping Spectroscopy. *Sci. Rep.* **2020**, *10* (1), 1–9.

(5) Chi, M.; Han, X.; Xu, Y.; Wang, Y.; Shu, F.; Zhou, W.; Wu, Y. An Improved Background-Correction Algorithm for Raman Spectroscopy Based on the Wavelet Transform. *Appl. Spectrosc.* **2019**, *73* (1), 78–87.